INTERNATIONAL JOURNAL FOR NUMERICAL METHODS IN FLUIDS, VOL. 10, 1–12 (1990)

FUNDAMENTAL SOLUTIONS OF THE STREAMFUNCTION–VORTICITY FORMULATION OF THE NAVIER–STOKES EQUATIONS

H. A. RODRIGUEZ-PRADA, F. F. PIRONTI AND A. E. SÁEZ

Departmento de Termodinamica y Fenómenos de Transferencia, Universidad Simón Bolívar, PO Box *89000, Caracas 1086–A, Venezuela*

SUMMARY

A new boundary element procedure is developed for the solution of the streamfunction–vorticity formulation of the Navier–Stokes equations in two dimensions. The differential equations are stated in their transient version and then discretized via finite differences with respect to time. In this discretization, the non-linear inertial terms are evaluated in a previous time step, thus making the scheme explicit with respect to them. In the resulting discretized equations, fundamental solutions that take into account the coupling between the equations are developed by treating the non-linear terms as inhomogeneities. The resulting boundary integral equations are solved by the regular boundary element method, in which the singular points are placed outside the solution domain.

KEY WORDS Fundamental solutions Navier–Stokes equations Regular boundary elements

INTRODUCTION

The boundary element method has gained wide acceptance in the treatment of partial differential equations. Its main advantage is that it allows one to find a solution of a specific problem only at the boundary of the domain, decoupling the boundary solution from the solution at interior points. The latter can be found *a posteriori* by direct integration. Because of this fact, the technique leads to a system of equations smaller than that obtained by conventional methods, when comparing the same degree of accuracy.[1]

In the field of fluid mechanics, the boundary element method has been recognized as a powerful technique for the solution of potential flow problems.[2–4] Its application to solve viscous flow problems has been explored in recent years. Examples of this are the works of Youngren and Acrivos[5] and Bush and Tanner,[6] in which inertial effects were neglected and the velocity–pressure formulation of the Navier–Stokes equations was considered. The inclusion of the inertial terms of the Navier–Stokes equations complicates the problem considerably. Bush[7] treated this problem in the velocity–pressure formulation by using a method of direct iteration to deal with the non-linearities.

The solution of the streamfunction–vorticity formulation of the Navier–Stokes equations in two dimensions via boundary elements has been performed in a limited number of works. Onishi *et al.*[8] and Farooq and Kuwabara[9] considered the time-dependent form of these equations. They used the fundamental solution of Poisson's equation to find the boundary integral equation of the streamfunction. On the other hand, the boundary integral equation of the vorticity was obtained

0271–2091/90/010001–12$06.00

Received 20 June 1988
Revised 24 February 1989

by using a time-dependent fundamental solution that considered the inertial terms in the vorticity equation as point sources. An explicit time-marching procedure was used, so that the non-linear terms in the equations added no further complication to the numerical technique.

Fundamental solutions have been found recently for incompressible viscous steady and unsteady flow problems via integral equation formulations with primitive variables.[10,11] In a previous work[12] the boundary element method for solving the steady-state Navier–Stokes equations in their streamfunction–vorticity formulation was presented. The method proposed there is based on the use of a new set of fundamental solutions that provide a complete coupling between the streamfunction and vorticity equations, thereby avoiding the usual problems that this formulation has in the treatment of boundary conditions in which both the streamfunction and its normal derivative are specified, as occurs in no-slip boundary conditions. The non-linear terms are considered as inhomogeneities in the development of the boundary integral equations and treated by direct iteration based on successive substitutions of newly calculated values. This technique becomes unstable for high Reynolds numbers. In this work we propose another set of new fundamental solutions starting from the non-steady-state Navier–Stokes equations in the streamfunction–vorticity formulation with complete coupling, but the treatment of the non-linear terms is done via a time discretization procedure.

MATHEMATICAL FORMULATION

The two-dimensional unsteady-state flow of an incompressible Newtonian fluid is governed by the Navier–Stokes equations which, when formulated in terms of the streamfunction (ψ) and the vorticity (ω), take the following form.

$$\nabla^2\psi = -\omega, \tag{1}$$

$$\nabla^2\omega = Re\left(\frac{\partial\psi}{\partial y}\frac{\partial\omega}{\partial x} - \frac{\partial\psi}{\partial x}\frac{\partial\omega}{\partial y}\right) + \frac{\partial\omega}{\partial t}. \tag{2}$$

These equations are stated in dimensionless form. The Reynolds number ($Re = \rho v_0 L/\mu$) is expressed in terms of a characteristic length L, with respect to which the two independent coordinates x and y have been made dimensionless, and a characteristic velocity v_0. Time is made dimensionless by using a characteristic time $t_0 = \rho L^2/\mu$.

By using a first-order time discretization for $\partial\omega/\partial t$, which introduces an error of order Δt, and letting the inertial terms be explicit while keeping the rest of the terms implicit, the differential equations (1) and (2) take the form

$$\nabla^2\omega_n = Re\left(\frac{\partial\psi_{n-1}}{\partial y}\frac{\partial\omega_{n-1}}{\partial x} - \frac{\partial\psi_{n-1}}{\partial x}\frac{\partial\omega_{n-1}}{\partial y}\right) + \frac{\omega_n - \omega_{n-1}}{\Delta t}, \tag{3}$$

$$\nabla^2\psi_n = -\omega_n. \tag{4}$$

In these equations the subscript n denotes the current time level and $n-1$ a previous time level, a time step Δt apart. We will consider the non-linear terms in equation (3) as inhomogeneities of the problem for the process of finding fundamental solutions. Based on this, equations (3) and (4) are reformulated as follows:

$$\nabla^2\omega_n - \alpha^2\omega_n = f_{n-1}, \tag{5}$$

$$\nabla^2\psi_n + \omega_n = 0, \tag{6}$$

where

$$\alpha^2 = 1/\Delta t, \tag{7}$$

$$f_{n-1} = Re\left(\frac{\partial\psi_{n-1}}{\partial y}\frac{\partial\omega_{n-1}}{\partial x} - \frac{\partial\psi_{n-1}}{\partial x}\frac{\partial\omega_{n-1}}{\partial y}\right) - \alpha^2\omega_{n-1}. \tag{8}$$

We then propose as fundamental solution of equation (5) a function F_ω that satisfies the following differential equation:

$$\nabla^2 F_\omega - \alpha^2 F_\omega = -\delta(\mathbf{r}-\boldsymbol{\xi}), \tag{9}$$

where δ is the Dirac delta function, $\mathbf{r}$ is a two-dimensional position vector in the x–y plane and $\boldsymbol{\xi}$ is an arbitrary vector locating the point at which the singularity of the delta function is placed.

The solution of equation (9) is the fundamental solution of the modified Helmholtz equation (details are given in the Appendix):

$$F_\omega(\mathbf{r};\boldsymbol{\xi}) = (1/2\pi)\{[C+\ln(\alpha/2)]\,I_0(\alpha\|\mathbf{r}-\boldsymbol{\xi}\|) + K_0(\alpha\|\mathbf{r}-\boldsymbol{\xi}\|)\}, \tag{10}$$

where C is Euler's constant, $\|\mathbf{r}-\boldsymbol{\xi}\|$ is the distance in the x–y plane between the points located by the vectors $\mathbf{r}$ and $\boldsymbol{\xi}$, and I_0 and K_0 are zeroth-order modified Bessel functions of the second kind.

Now we will seek a fundamental solution of equation (6), F_ψ, that satisfies the following singular inhomogeneous problem.

$$\nabla^2 F_\psi + F_\omega = -\delta(\mathbf{r}-\boldsymbol{\xi}). \tag{11}$$

This equation can be integrated by formulating it in polar co-ordinates with origin at the point located by the vector $\boldsymbol{\xi}$ (see Appendix). The result is

$$F_\psi(\mathbf{r};\boldsymbol{\xi}) = -(1/2\pi\alpha^2)\{(1+\alpha^2)\ln\|\mathbf{r}-\boldsymbol{\xi}\| + [C+\ln(\alpha/2)]\,I_0(\alpha\|\mathbf{r}-\boldsymbol{\xi}\|) + K_0(\alpha\|\mathbf{r}-\boldsymbol{\xi}\|)\}. \tag{12}$$

The fundamental solutions given by equations (10) and (12) will allow the development of the boundary integral form of the differential equations (5) and (6). Multiplying equation (9) by ω_n, equation (5) by F_ω and subtracting yields

$$F_\omega\nabla^2\omega_n - \omega_n\nabla^2 F_\omega = F_\omega f_{n-1} + \omega_n\delta(\mathbf{r}-\boldsymbol{\xi}). \tag{13}$$

This equation can be integrated over the solution domain Ω (Figure 1). Performing this and

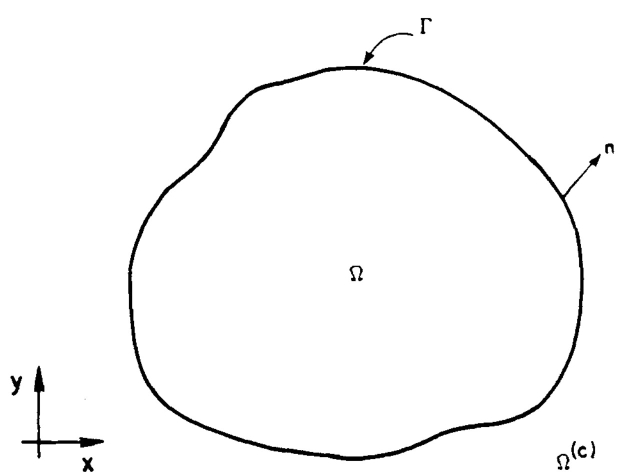

Figure 1. Solution domain

applying Green's theorem leads to

$$\int_{\Gamma}\left(F_{\omega}\frac{\partial \omega_n}{\partial n}-\omega_n\frac{\partial F_{\omega}}{\partial n}\right)\mathrm{d}\Gamma=\int_{\Omega}F_{\omega}f_{n-1}\,\mathrm{d}\Omega+a(\xi)\omega_n(\xi), \tag{14}$$

where the integrations are performed with respect to $\mathbf{r}$ and where Γ is the boundary of Ω. The parameter $a(\xi)$ is a geometric factor resulting from the integration of the delta function. It can be shown that it takes on the following values, depending on the location of ξ.

$$a(\xi)=\begin{Bmatrix}1 & \text{if } \xi\in\Omega \\ 0 & \text{if } \xi\in\Omega^{(c)}, \\ \theta/2\pi & \text{if } \xi\in\Gamma.\end{Bmatrix} \tag{15}$$

In this equation $\Omega^{(c)}$ represents the exterior of the domain, excluding its boundaries, and θ is the angle formed between tangents to the boundary at point ξ, approaching it from each side, as illustrated in Figure 2. Note that, for points at which the boundary is a differentiable curve, $\theta=\pi$.

Equation (14) will be taken as the boundary integral form of equation (5). To find the boundary integral equation corresponding to equation (6), consider first the equation formed by combining equations (5) and (6), namely

$$\alpha^2\nabla^2\psi_n+\nabla^2\omega_n=f_{n-1}. \tag{16}$$

Furthermore, considering the combination of equations of (9) and (11), we have

$$\nabla^2F_{\omega}+\alpha^2\nabla^2F_{\psi}=-(1+\alpha^2)\delta(\mathbf{r}-\xi). \tag{17}$$

Then equation (16) is multiplied by F_{ω} and F_{ψ} and equation (17) by ω_n and ψ_n to obtain the following equations:

$$\alpha^2F_{\omega}\nabla^2\psi_n+F_{\omega}\nabla^2\omega_n=F_{\omega}f_{n-1}, \tag{18}$$

$$\alpha^2F_{\psi}\nabla^2\psi_n+F_{\psi}\nabla^2\omega_n=F_{\psi}f_{n-1}, \tag{19}$$

$$\omega_n\nabla^2F_{\omega}+\alpha^2\omega_n\nabla^2F_{\psi}=-(1+\alpha^2)\delta(\mathbf{r}-\xi)\omega_n, \tag{20}$$

$$\psi_n\nabla^2F_{\omega}+\alpha^2\psi_n\nabla^2F_{\psi}=-(1+\alpha^2)\delta(\mathbf{r}-\xi)\psi_n. \tag{21}$$

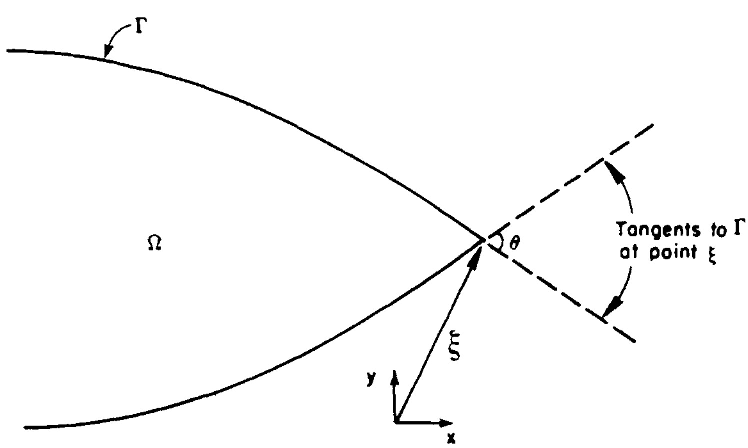

Figure 2. Evaluation of θ

Now the following combination is performed with the last equations, (18) + α^2(19) − (20) − α^2(21), to obtain, after some simplifications and using equation (13),

$$(F_\omega \nabla^2 \psi_n - \psi_n \nabla^2 F_\omega) + \alpha^2 (F_\psi \nabla^2 \psi_n - \psi_n \nabla^2 F_\psi) + (F_\psi \nabla^2 \omega_n - \omega_n \nabla^2 F_\psi) = F_\psi f_{n-1} + [(1+\alpha^2)\psi_n + \omega_n]\delta(\mathbf{r} - \boldsymbol{\xi}). \tag{22}$$

Finally, integrating this equation over Ω and applying Green's theorem leads to a second boundary integral equation.

$$\int_\Gamma \left(F_\omega \frac{\partial \psi_n}{\partial n} - \psi_n \frac{\partial F_\omega}{\partial n} + \alpha^2 F_\psi \frac{\partial \psi_n}{\partial n} - \alpha^2 \psi_n \frac{\partial F_\psi}{\partial n} + F_\psi \frac{\partial \omega_n}{\partial n} - \omega_n \frac{\partial F_\psi}{\partial n} \right) \mathrm{d}\Gamma = \int_\Omega F_\psi f_{n-1} \, \mathrm{d}\Omega + a(\boldsymbol{\xi})[(1+\alpha^2)\psi_n(\boldsymbol{\xi}) + \omega_n(\boldsymbol{\xi})]. \tag{23}$$

The integrodifferential equations (14) and (23) represent a formulation equivalent to the original problem (equations (5) and (6)). Providing that $f(\mathbf{r})$ is a known function, equations (14) and (23) have the useful characteristic that, when evaluated at points $\boldsymbol{\xi}$ on the boundary Γ or in $\Omega^{(c)}$, they interrelate the values of the dependent variables and their derivatives on the boundaries, thus allowing the evaluation of a boundary solution.

Equations (14) and (23) can be discretized following the regular boundary element approach.[6] The integrals over Γ in those equations are expressed as the sum of the integrals over a grid of linear boundary elements. Posteriorly, the dependent variables (ψ_n and ω_n) and their normal derivatives ($\partial \psi_n / \partial n$ and $\partial \omega_n / \partial n$) are expressed as linear functions within each element. The descretized forms of equations (14) and (23) are thus formulated in terms of the nodal values of ψ_n, ω_n, $\partial \psi_n / \partial n$ and $\partial \omega_n / \partial n$. After substituting the known boundary conditions for the streamfunction and vorticity (assumed to be of the Dirichlet or Neumann type), the resulting equations contain $2N$ unknowns, where N is the total number of nodes of the boundary element grid. Afterwards, we define N singular points, $\boldsymbol{\xi}_1$, located on a vector normal to Γ at a distance equal to the mean length of adjacent elements. This allows us to generate $2N$ algebraic equations. The result of the process is a system of equations that can be expressed in the following way:

$$\mathbf{A}\mathbf{x} = \mathbf{b} + \mathbf{q}, \tag{24}$$

where $\mathbf{A}$ is a $2N \times 2N$ matrix and $\mathbf{x}$ is the vector of unknowns, containing $2N$ elements which are the unspecified boundary values of ψ_n, ω_n, $\partial \psi_n / \partial n$ and $\partial \omega_n / \partial n$. The vector $\mathbf{b}$ is formed by the terms of the integrals in equations (14) and (23) that can be evaluated from the boundary conditions, and $\mathbf{q}$ has elements which correspond to the integrals over Ω in equations (14) and (23).

Once the geometry of the discretization and the boundary conditions are specified, the matrix $\mathbf{A}$ and the vector $\mathbf{b}$ are completely determined. On the other hand, a knowledge of the solution in the interior of the domain is required to evaluate the vector $\mathbf{q}$, since f_{n-1} (equation (8)) depends on it. To find the solution to the problem, the following procedure may be used.

1. Start from an initial estimate for $\mathbf{q}$ and fix a value for the time step Δt.
2. Form the matrix $\mathbf{A}$ and vector $\mathbf{b}$.
3. Find the inverse matrix $\mathbf{A}^{-1}$.
4. Calculate $\mathbf{x}$ from

$$\mathbf{x} = \mathbf{A}^{-1}(\mathbf{b} + \mathbf{q}).$$

5. Calculate the solution in the interior of the domain from equations (14) and (23) evaluated at interior points. Calculate the new vector $\mathbf{q}$.

6. Stop if the maximum absolute deviation of nodal values of streamfunction, vorticity and their normal derivatives between the current and the previous time steps is below a specified tolerance. Otherwise, return to step 4.

There are two important features to point out from the solution scheme employed. First, the solution of the system of equations has to be performed only once, since the inverse matrix $\mathbf{A}^{-1}$ can be stored and used subsequently. This can be done because $\mathbf{A}$ is only a function of the geometry of the discretization. Secondly, in the system of equations (16) there is a complete coupling among all the dependent variables. This is the most important characteristic of the method developed in this work and what makes it different from conventional finite and boundary element algorithms, which in general require a special treatment of boundaries in which there are two specifications for the streamfunction and none for the vorticity.

APPLICATION

To illustrate the application of the method presented in the preceding section, consider the flow inside a square cavity whose upper lid is moving at a constant velocity. The geometry and boundary conditions for this problem are shown in Figure 3. The results corresponding to

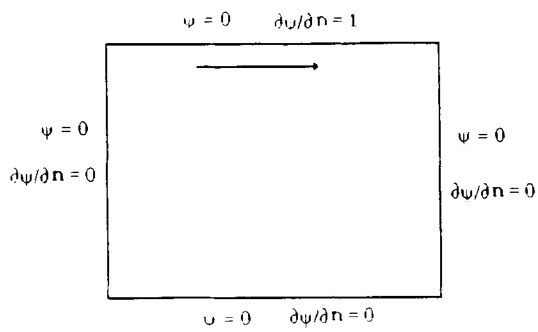

Figure 3. Flow inside a square cavity

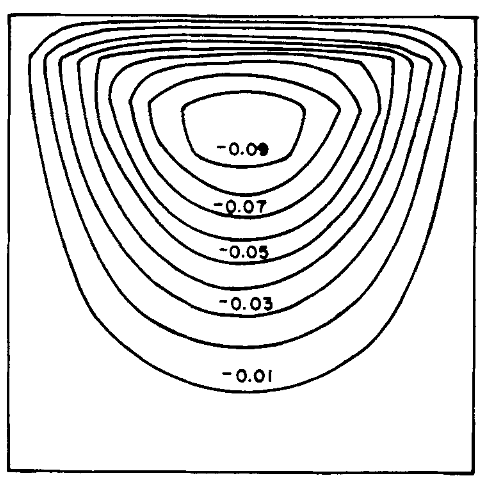

Figure 4. Streamlines for flow in a square cavity, $Re=0$

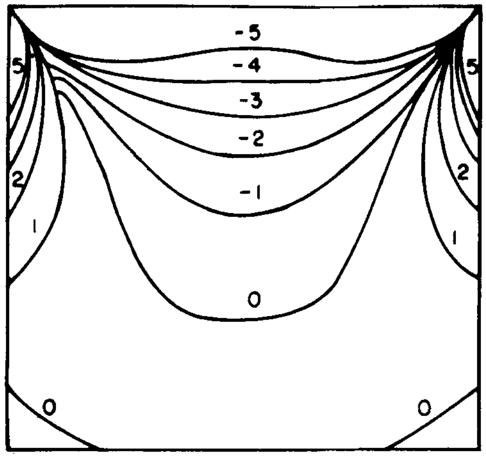

Figure 5. Constant–vorticity lines for flow in a square cavity, $Re=0$

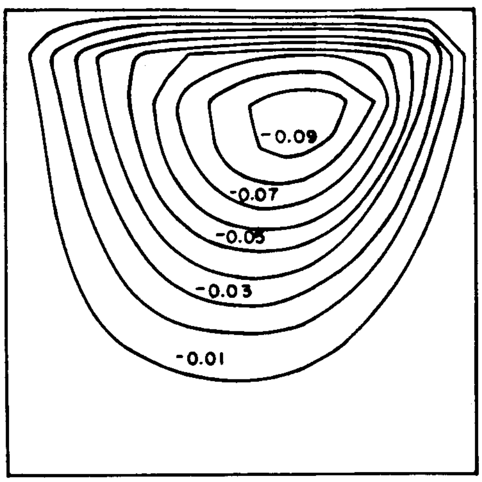

Figure 6. Streamlines for flow in a square cavity, $Re=100$

Reynolds numbers of 0, 100 and 200 are shown in Figures 4–9. These results were obtained by using a grid of 64 boundary nodes and with the fundamental solution corresponding to $\alpha = 0$, a case for which the iterative procedure becomes a direct iteration since the values of the non-linear terms in each iteration correspond directly to the evaluation of those terms from the results of the previous iteration.

The results for $Re = 0$, shown in Figures 4 and 5, did not require iteration because in this case $f=0$ and therefore $\mathbf{q}=\mathbf{0}$, which turns equation (16) into a linear system. We point out that other conventional boundary element algorithms for the streamfunction–vorticity equations require an iterative procedure even for $Re=0$, since in the application considered the boundary conditions are all imposed on the streamfunction. The coupling between the two basic differential equations that provides the algorithm developed in this work allows a direct solution of the case $Re=0$. This

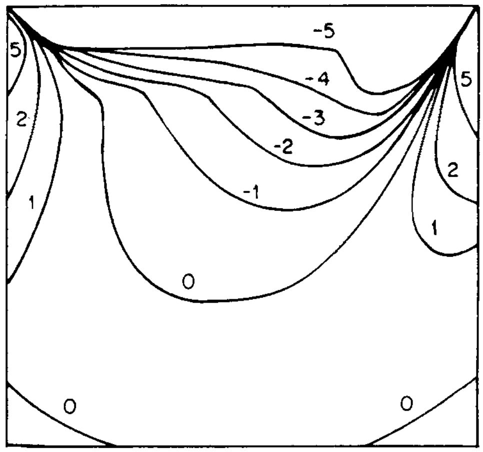

Figure 7. Constant-vorticity lines for flow in a square cavity, $Re=100$

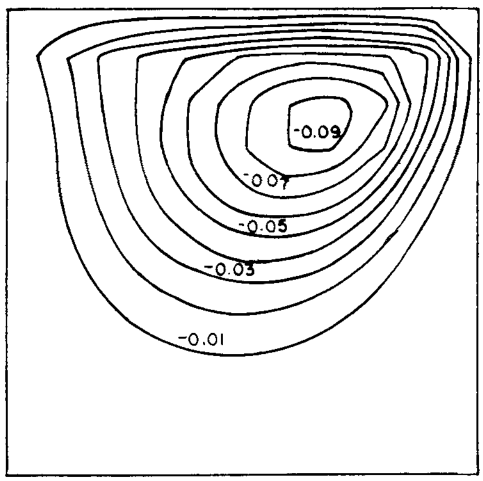

Figure 8. Streamlines for flow in a square cavity, $Re=200$

is an important advantage of the method since it can handle virtually all the types of boundary conditions encountered in practice.

The results obtained are similar to those reported by Farooq and Kuwabara[9] to the point that the contour plots are exactly the same at the scale of the figures. Furthermore, the location of the centre of the primary vortex as well as the magnitudes of the streamfunction and vorticity agree with those reported in the works of Nallasamy and Prasad[13] and Gupta and Manohar,[14] as illustrated in Table I.

The algorithm used in this work did not converge for Reynolds numbers larger than 300, even using relaxation between iterations. The relaxation scheme employed consisted of modifying the values of the boundary unknowns (x) predicted by the iterative procedure by the following equation:

$$\mathbf{x}=\beta\mathbf{x}^{(k)}+(1-\beta)\,\mathbf{x}^{(k-1)},$$

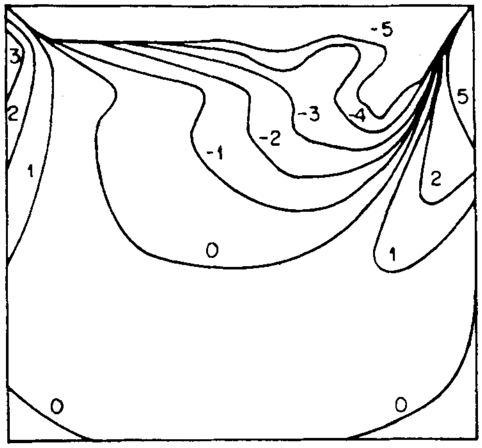

Figure 9. Constant-vorticity lines for flow in a square cavity, $Re=200$

Table I. Comparison of results with previous works

	Location of vortex centre		Value of $-\psi$ at vortex centre		Value of ω at vortex centre	
Re	Ref. 14	This work	Ref. 14	This work	Ref. 14	This work
0	0·50, 0·75	0·50, 0·75	0·092–0·101	0·099	4·9–6·0	4·8
100	0·37, 0·75	0·38, 0·75	0·081–0·100	0·095	6·3–8·6	6·5

where $\mathbf{x}^{(k)}$ and $\mathbf{x}^{(k-1)}$ are the values predicted in iterations k and $k-1$ respectively and $\mathbf{x}$ is the real value of the vector used to evaluate the vector $\mathbf{q}$ for the next iteration. The relaxation parameter β was varied between 0 and 1 with no consequence over the convergence limit of $Re=300$.

The limitation of convergence at high Reynolds numbers was expected, since the iterative procedure is a direct iteration based on successive substitutions of newly calculated values of f and this technique has proved to be unstable for high Reynolds numbers in other algorithms.[14] However, it might be possible that results obtained by using fundamental solutions generated by changing the values of the parameter α converge for larger Reynolds numbers. This aspect of the investigation is being explored at the present time.

Finally, it is important to point out that the technique used in the present work yields high accuracy with respect to the size of the grid employed. It has been mentioned that the results presented in Figures 4–9 correspond to 64 boundary nodes. However, in terms of the accuracy that can be perceived from the plots, the results corresponding to 32 boundary nodes are indistinguishable from those presented. Figure 10 shows a comparison of the vorticity values at the upper lid obtained by using 32 and 64 boundary nodes. Although there are some differences between them, the profiles only differ significantly near the corners, where the vorticity has a singularity. The internal solution is not sensitive to those differences up to the third significant digit. Since the upper-lid vorticity represents the part of the solution that converges more slowly to the exact solution, it can be concluded that 32 boundary nodes are enough to obtain an accurate solution.

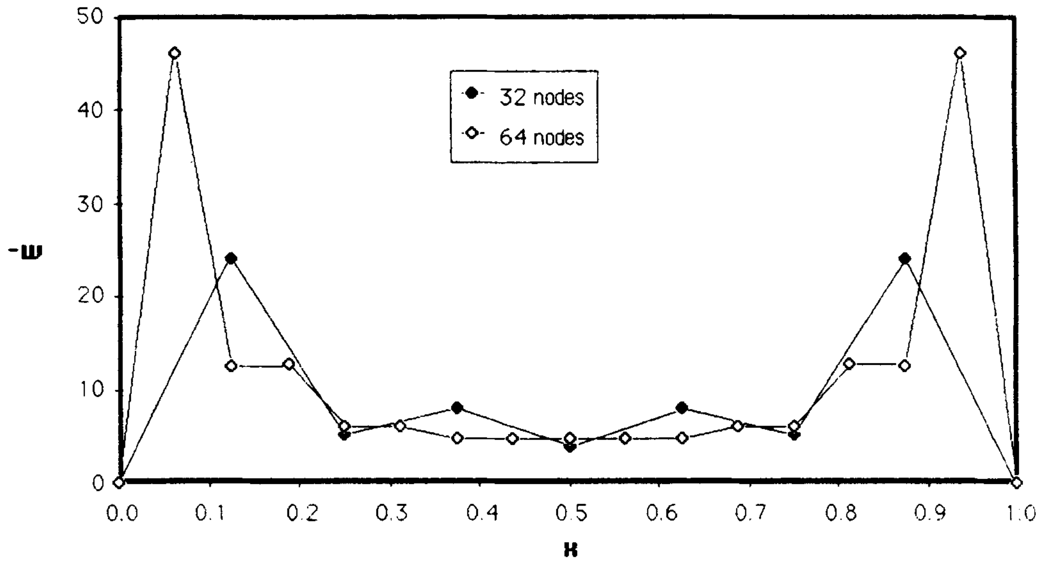

Figure 10. Values of the vorticity at the upper lid, $Re=0$

CONCLUSIONS

The boundary element method is applied to solve the streamfunction–vorticity formulation of the Navier–Stokes equations. The procedure developed relies on the use of fundamental solutions that take into account the coupling between the differential equations through the vorticity term in the streamfunction equation. The non-linear terms are considered as inhomogeneities in the development of the boundary integral equations and treated by means of a time discretization procedure. The formulation allows one to handle no-slip boundary conditions in a direct manner, avoiding iteration to find the vorticity values on no-slip boundaries. The discretization of the resulting boundary integral equations can be performed by placing the singular points outside the solution domain, as is done in the regular boundary element method.

APPENDIX

We present the procedure for the derivation of the fundamental solutions given by equations (10) and (12). In general, a fundamental solution of a second-order singular equation can be obtained by performing the following steps:

1. Solve the homogeneous problem, expressing the solution in terms of two integration constants.
2. Force the homogeneous problem solution to satisfy the integral form of the singular equation, thus finding one of the integration constants.
3. Set the value of the second integration constant arbitrarily.

Fundamental solution of equation (9)

By using cylindrical co-ordinates and taking $r=\|\mathbf{r}-\boldsymbol{\xi}\|$ we obtain the homogeneous form of equation (9),

$$\frac{1}{r}\frac{\mathrm{d}}{\mathrm{d}r}\left(r\frac{\mathrm{d}F_{\omega}}{\mathrm{d}r}\right)-\alpha^{2}F_{\omega}=0.. \tag{25}$$

The general solution of this problem is

$$F_\omega(r) = AI_0(\alpha r) + BK_0(\alpha r). \tag{26}$$

On the other hand, the integration of equation (9) over a circle of radius r yields, after applying the divergence theorem and remembering that the integral of the Dirac delta function over a domain surrounding its singularity is equal to one,

$$2\pi r \frac{\mathrm{d}F_\omega}{\mathrm{d}r} - 2\pi\alpha^2 \int_0^r F_\omega r \,\mathrm{d}r = -1. \tag{27}$$

Substituting equation (26) into equation (27) yields $B = 1/2\pi$, from which equation (26) becomes

$$F_\omega(r) = AI_0(\alpha r) + (1/2\pi)\,K_0(\alpha r). \tag{28}$$

This is the most general form of the fundamental solution. The constant A must be specified and it can have any arbitrary value. In this work we will choose this constant so that equation (28) reduces, as $\alpha \to 0$, to the following solution, found in a previous work:[12]

$$F_\omega = -(1/2\pi)\ln r. \tag{29}$$

Using series expansions for the Bessel functions, taking the limit in equation (28) and equating the result to equation (29) leads to

$$A = (1/2\pi)\,[\ln(\alpha/2) + C], \tag{30}$$

where C is Euler's constant. The resulting fundamental solution is given by equation (10).

Fundamental solution of equation (11)

By using cylindrical co-ordinates, taking $r = \|\mathbf{r} = \boldsymbol{\xi}\|$ and using equation (28) we obtain the homogeneous form of equation (11),

$$\frac{1}{r}\frac{\mathrm{d}}{\mathrm{d}r}\left(r\frac{\mathrm{d}F_\psi}{\mathrm{d}r}\right) + AI_0(\alpha r) + \frac{1}{2\pi}K_0(\alpha r) = 0. \tag{31}$$

The general solution of this problem is

$$F_\psi(\alpha r) = -\frac{A}{\alpha^2} I_0(\alpha r) - \frac{1}{2\pi\alpha^2} K_0(\alpha r) + E\ln r + D, \tag{32}$$

where E and D are the constants of integration.

Integrating equation (11) over a circle of radius r yields

$$2\pi r\,\mathrm{d}F_\psi/\mathrm{d}r + 2\pi \int_0^r F_\omega r\,\mathrm{d}r = -1. \tag{33}$$

Substituting equations (28) and (32) into equation (33) leads to

$$E = -\frac{1}{2\pi}\frac{1+\alpha^2}{\alpha^2}. \tag{34}$$

With the use of this relation, equation (32) represents the most general fundamental solution of the problem. The constant D is arbitrarily set equal to zero and thus equation (12) is obtained. With this choice, as $\alpha \rightarrow 0$, it can be shown that equation (32) becomes

$$F_{\psi} = \frac{1}{2\pi}\left(\frac{r^2}{4} - 1\right)\ln r - \frac{r^2}{8\pi}, \tag{35}$$

which was derived in a previous work.[12]

REFERENCES

1. C. A. Brebbia, 'The boundary element method in engineering practice', in C. A. Brebbia (ed.), *Boundary Element Research*, CML Publications, Southampton, 1985.
2. C. A. Brebbia, *The Boundary Element Method for Engineers*, Pentech Press, London, 1978.
3. C. A. Brebbia and L. C. Wrobel, 'Boundary element method for fluid flow', in C. A. Brebbia (ed.), *Boundary Element Research*, CML Publications, Southampton, 1985.
4. C. Patterson and M. A. Sheikh, 'A regular boundary element method for fluid flow', *Int. j. numer. methods fluids*, **2,** 239 (1982)
5. G. K. Youngren and A. J. Acrivos, 'Stokes flow past a particle of arbitrary shape: a numerical method of solution', *J. Fluid Mech.*, **69,** 377 (1975).
6. M. B. Bush and R. I. Tanner, 'The boundary element method applied to a creeping motion of a sphere', paper presented at the *2nd Int. Conf. on Numerical Methods in Laminar and Turbulent Flows*, Venice, 1981.
7. M. B. Bush, 'Modelling two-dimensional flow past arbitrary cylindrical bodies using boundary element formulations', *Appl. Math. Model.*, **7,** 386 (1983).
8. K. Onishi, T. Kuroki and M. Tanaka, 'An application of boundary element method to incompressible laminar viscous flow', *Eng. Anal.*, **1,** 122 (1984).
9. M. U. Farooq and S. Kuwabara, 'Analysis of the unsteady Navier–Stokes equations based on Green's function approach', *J. Phys. Soc. Japan*, **53,** 1702 (1984).
10. N. Tosaka and K. Kakuda, 'Integral equation formulations with the primitive variables for incompressible viscous flow problems', in M. Tanaka and C. A. Brebbia (eds), *Boundary Elements VIII*, Springer–Verlag, New York, 1986.
11. J. C. Wu, 'Fundamental solutions and boundary element methods', *Eng. Anal.*, **4,** 2 (1987).
12. H. A. Rodriguez-Prada and A. E. Sáez, 'A boundary element solution of the stream function–vorticity formulation of the Navier–Stokes equations', in C. Taylor and M. M. Hafez (eds), *Numerical Methods in Laminar and Turbulent Flow, Vol. V*, Pineridge Press, Swansea, 1987.
13. M. Nallasamy and K. Krishna Prasad, 'On cavity flow at high Reynolds numbers', *J. Fluid Mech.*, **70,** 391 (1977).
14. M. M. Gupta and R. P. Manohar, 'Boundary approximations and accuracy in viscous flow computations', *J. Comput. Phys.*, **31,** 265 (1979).